

# DiffTune: Auto-Tuning through Auto-Differentiation

Sheng Cheng, Minkyung Kim\*, Lin Song\*, Zhuohuan Wu, Shenlong Wang, and Naira Hovakimyan

**Abstract**—The performance of a robot controller depends on the choice of its parameters, which require careful tuning. In this paper, we present DiffTune, a novel, gradient-based automatic tuning framework. Our method unrolls the dynamical system and controller as a computational graph and updates the controller parameters through gradient-based optimization. Unlike the commonly used back-propagation scheme, the gradient in DiffTune is obtained through sensitivity propagation, a forward-mode auto differentiation technique that runs parallel to the system’s evolution. We validate the proposed auto-tune approach on a Dubin’s car and a quadrotor in challenging simulation environments. Simulation experiments show that the approach is robust to uncertainties in the system dynamics and environment and generalizes well to unseen trajectories in tuning.

## I. INTRODUCTION

Robots’ execution of complicated tasks builds upon low-level controllers that deliver precise and responsive motions. Controller design requires qualitative analysis to ensure stability and then parameter tuning to deliver the designed performance on real systems. Controller tuning is normally done by hand, by either trial-and-error or proven methods for specific controllers (e.g., Ziegler–Nichols method for proportional-integral-derivative (PID) controller tuning [1]). However, hand-tuning often requires experienced personnel and can be inefficient, especially for systems with long loop times or a huge parameter space.

To improve the efficiency and performance, automatic tuning (or auto-tune) methods have been investigated. Such methods integrate system knowledge, expert experience, and software tools to determine the best set of controller parameters, especially for the widely used PID controllers [2]–[4]. Commercial auto-tune products have been available since 1980s [3], [5]. A desirable auto-tune scheme should have the following three qualities: i) stability of the target system; ii) compatibility with real systems’ data; and iii) efficiency for online deployment, possibly in real-time. However, how to design the auto-tune scheme, simultaneously having the above three qualities, for general controllers is still a challenge.

Existing auto-tune methods can be categorized into model-based [6], [7] and model-free [8]–[13]. Both approaches iteratively select the next set of parameters for evaluation that is likely to improve the performance than the previous

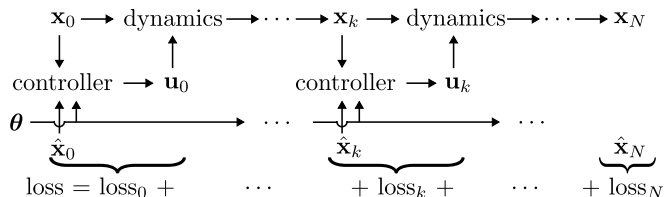


Fig. 1: Illustration of an unrolled dynamical system as a computational graph. The summed loss is the root node, whereas the parameter  $\theta$  is the leaf node.

attempts. Model-based auto-tune methods leverage knowledge of the system model to improve performance, often using the gradient of the performance criterion (e.g., tracking error) and applying gradient descent so that the performance can improve based on the local gradient information [6], [7]. Stability can be ensured through explicitly leveraging knowledge about the system dynamics. However, model-based auto-tune might not work in real environment, where the knowledge about the dynamical model might be imperfect. This issue is especially severe when controller parameters are tuned in simulation and then deployed to a real system.

Model-free auto-tune methods approximate gradient or a surrogate model to improve the performance. Representative approaches include Markov chain Monte Carlo [12], Gaussian process (GP) [8]–[11], deep neural network (DNN) [13], etc. Such approaches often make no assumptions on the model and have the advantage in real-data compatibility owing to their data-driven nature. However, some model-free approaches, such as GPs [14], are inefficient when tuning in high-dimensional parameter spaces. Besides, it is hard to establish stability guarantees with data-driven methods, where empirical methods are often applied.

To overcome the challenges in the auto-tune scheme, we present *DiffTune*: an auto-tune method based on auto-differentiation. Our method is inspired by the “end-to-end” idea from the learning community. Specifically, in the proposed scheme, the gradient of the loss function (evaluating the performance of the controller) with respect to the controller parameters can be directly obtained and then applied to gradient-descent to improve the performance. *DiffTune* is generally applicable to tune all the controller parameters as long as the system dynamics and controller are differentiable (we will define “differentiable” in Section III), which is the case with most of the systems. For example, algebraically computed controllers, e.g., with the structure of gain-times-error (PID [7]), are differentiable. Moreover, following the seminal work [15] that differentiates the  $\text{argmin}$  operator using the Implicit Function Theorem, one can see that controllers relying on solutions of an optimization problem

\*These authors contributed equally to this work.

S. Cheng, M. Kim, L. Song, Z. Wu, and N. Hovakimyan are with the Department of Mechanical Science and Engineering, and S. Wang is with the Department of Computer Science. All authors are with the University of Illinois Urbana-Champaign, USA. (email: {chengs, mk58, linsong2, zw24, shenlong, nhovakim}@illinois.edu)

to generate control actions (e.g., model predictive control (MPC) [16], [17], optimal control [18], [19], control barrier function [20]–[23], linear-quadratic regulator (LQR) [24]) are also differentiable.

We build *DiffTune* by treating the unrolled dynamical system as a computational graph and then apply auto-differentiation to compute the gradient. Unlike the commonly used back-propagation scheme, we present an equivalent way of computation, called sensitivity propagation, which propagates the gradient in the forward direction in parallel to the dynamics’ propagation. The sensitivity propagation is based on the sensitivity equation [25] for nonlinear dynamical system. The unique aspect of the sensitivity propagation lies in its capability to incorporate real systems’ data, in which case the computational graph is broken because the new system states are obtained through sensor measurements or state estimation instead of evaluating those from the dynamics. On the contrary, the broken computational graph forbids the usage of reverse-mode auto-differentiation, making sensitivity propagation the preferred approach.

*DiffTune* enjoys the earlier mentioned three qualities simultaneously: **stability** is inherited from the controllers with stability guarantees by design; **real-data compatibility** is enabled by the sensitivity propagation; and **efficiency** is provided since the sensitivity propagation runs forward in time and in parallel to the system’s evolution.

**Our contributions are summarized as follows:** i) We propose an auto-tuning method for controller parameters over general dynamical systems and controllers that are differentiable by unrolling into a computational graph and applying reverse-mode auto-differentiation; ii) We develop the sensitivity propagation (analytically equivalent to reverse-mode auto-differentiation) that can incorporate data from real systems for auto-tuning, enabling the method to be implemented online.

The remainder of the paper is organized as follows: Sections II and III review related work and background, respectively, of this paper. Section IV describes our auto-tuning method with a comparison between reverse-mode auto-differentiation and sensitivity propagation. We also discuss uncertainty handling when using real system data. Section V shows the simulation results on a Dubins’ car and on a quadrotor. Finally, Section VI concludes the paper.

## II. RELATED WORK

Our approach closely relates to classical work on automatic parameter tuning and recent learning-based controllers. In this section, we briefly review previous work in these two major directions.

**Model-based auto-tune** leverages model knowledge to infer the parameter choice for performance improvement. In [6], an auto-tune method is proposed for LQR. Gradient of a loss function with respect to the parameterized quadratic matrix coefficients are approximated using Simultaneous Perturbation Stochastic Approximation [26]. In [7], the gradient of a quadratic loss over input control actions and system

outputs with respect to PID gains is computed using auto-differentiation tools.

**Model-free auto-tune** relies on zeroth-order approximate gradient or surrogate performance model to decide the new candidate parameters. In [27], the authors use extremum seeking to sinusoidally perturb the PID gains and then estimate the gradient. Gradient-free methods, e.g., Metropolis-Hastings sampling [12], have also been used for tuning. In terms of surrogate model, machine learning tools have been frequently used for their advantages in incorporating data. In [28], an end-to-end, data-driven hyperparameter tuning is applied to an MPC using a surrogate dynamical model. Besides, GP is often used as a non-parametric model that approximates an unknown function from input-output pairs with probabilistic confidence measures. This property makes GP a suitable surrogate model that approximates the performance function with respect to the tuned parameters. In [8], GP is applied to approximate the unknown cost function using noisy evaluations and then induce the probability distribution of the parameters that minimize the loss. In [9], the authors use GP to approximate the cost map over controller parameters while constructing safe sets of parameters to ensure safe exploration. Similar ideas have been applied to gait optimization for bipedal walking, where GP is used to approximate the cost map of parameterized gaits [10], [11]. Besides GP, DNNs [13] have also been used for model-free tuning.

**Learning for control** is a recently trending research direction that strives to combine the advantages of model-driven control and data-driven learning for safe operation of a robotic system. Exemplary approaches include, but not limited to, the following: reinforcement learning [29], [30], whose goal is to find an optimal policy while gathering data and knowledge of the system dynamics from interactions with the system; imitation learning [31], which aims to mimic the actions taken by a superior controller while making decisions using less information of the system than the superior controller; and iterative learning control [32], [33], which constructs the present control action by exploiting every possibility to incorporate past control and system information, typically for systems working in a repetitive mode. A recent survey [34] provides a thorough review on the safety aspect of learning for control in robotics.

## III. BACKGROUND

Consider a discrete-time dynamical system

$$\mathbf{x}_{k+1} = f(\mathbf{x}_k, \mathbf{u}_k), \quad (1)$$

where  $\mathbf{x}_k \in \mathbb{R}^n$  and  $\mathbf{u}_k \in \mathbb{R}^m$  are the state and control, respectively, and the initial state  $\mathbf{x}_0$  is known. The control is generated by a feedback controller that tracks a desired state  $\hat{\mathbf{x}}_k \in \mathbb{R}^n$  such that

$$\mathbf{u}_k = h(\mathbf{x}_k, \hat{\mathbf{x}}_k, \boldsymbol{\theta}), \quad (2)$$

where  $\boldsymbol{\theta} \in \mathbb{R}^p$  denotes the parameters of the controller, e.g.,  $\boldsymbol{\theta} \in \mathbb{R}^2$  may represent the P- and D-gain in a PD controller. We assume that the state  $\mathbf{x}_k$  can be measured directly or, if

not, an appropriate state estimator is used. Furthermore, we assume the dynamics (1) and controller (2) are differentiable, i.e., the Jacobians  $\nabla_{\mathbf{x}}f$ ,  $\nabla_{\mathbf{u}}f$ ,  $\nabla_{\mathbf{x}}h$ , and  $\nabla_{\theta}h$  exist, which widely applies to general systems.

The tuning task adjusts  $\theta$  to minimize an evaluation criterion, denoted by  $L(\cdot)$ , which is a function of the desired states, actual states, and control actions over a time interval of length  $N$ . An illustrative example is the quadratic loss of the deviation of the state to the desired state and control-effort penalty, where  $L(\mathbf{x}_{1:N}, \hat{\mathbf{x}}_{1:N}, \mathbf{u}_{0:N-1}; \theta) = \sum_{k=1}^N \|\mathbf{x}_k - \hat{\mathbf{x}}_k\|^2 + \sum_{k=0}^{N-1} \lambda \|\mathbf{u}_k\|^2$  with  $\lambda > 0$  being the penalty coefficient. We will use the short-hand notation  $L(\theta)$  for conciseness in the rest of the paper.

#### IV. METHOD

*DiffTune* gradually improves the system performance by tuning the controller parameters using gradient descent. We unroll the dynamical system (1) and controller (2) into a computational graph. Figure 1 illustrates the unrolled system, which stacks the iterative procedure of state update via the “dynamics” and control-action generation via the “controller.” We then use gradient-based methods to update the parameters  $\theta$ . Specifically, since the controller is stable for  $\theta$  within the feasible set  $\Theta$ , we use the projected gradient descent [35] to update  $\theta$  (and ensure stability):

$$\theta \leftarrow P_{\Theta}(\theta - \alpha \nabla_{\theta} L), \quad (3)$$

where  $P_{\Theta}$  is the projection operator that projects its operand into the set  $\Theta$  and  $\alpha$  is the step size. What remains to be done is to compute the gradient  $\nabla_{\theta} L$ , for which we provide two methods: backward propagation and sensitivity propagation.

Our method is inspired by the backward propagation used in training a neural network (NN): once the structure of the NN and loss function are defined, then the parameters of the NN are updated via gradient descent. Denote the NN parameters by  $\phi$  and the loss function by  $l(\phi)$ . Backward propagation, also known as the reverse-mode auto-differentiation on a computational graph, is nowadays used to obtain the gradient  $\nabla_{\phi} l$ . Likewise, the computational graph in Fig. 1 has the controller parameters  $\theta$  as the leaf node and the loss  $L(\theta)$  to be the root node, whereas all the intermediate states and control actions are non-leaf nodes. The computational graph has to be propagated forward first, with the value of each non-leaf node stored in the memory. Then the backward propagation uses chain rule and the stored non-leaf nodes in the memory to trace the graph from root to leaves and compute the desired gradient  $\nabla_{\theta} L$ . Backward propagation can be conveniently implemented using off-the-shelf tools like PyTorch [36] or TensorFlow [37]: one will program the forward pass on the computational graph using the dynamics and controller and set the parameters with respect to which the loss function will be differentiated.

However, backward propagation cannot incorporate data from real systems, because all the computation relies on a computation graph. Specifically, the dynamics (1) have to be evaluated each time to obtain a new state, which is not the case in real systems: the states are obtained through sensor

measurements or state estimation, instead of evaluating the dynamics. Thus, backward propagation can only be applied to controller tuning in simulations, forbidding the usage of real systems’ data. We introduce the sensitivity propagation next to address the issue of real-data compatibility.

##### A. Sensitivity propagation

Sensitivity propagation is an alternative method to compute  $\nabla_{\theta} L$ , whose output is analytically equivalent to that of back propagation on a computational graph. To see how sensitivity propagation works, we first break down the derivative  $\nabla_{\theta} L$  by

$$\nabla_{\theta} L = \sum_{k=1}^N \frac{\partial L}{\partial \mathbf{x}_k} \frac{\partial \mathbf{x}_k}{\partial \theta} + \sum_{k=0}^{N-1} \frac{\partial L}{\partial \mathbf{u}_k} \frac{\partial \mathbf{u}_k}{\partial \theta}. \quad (4)$$

Since  $\partial L / \partial \mathbf{x}_k$  and  $\partial L / \partial \mathbf{u}_k$  can be evaluated once  $L$  is chosen and  $\mathbf{x}_k$  and  $\mathbf{u}_k$  are known, what remains to be done is to formulate  $\partial \mathbf{x}_k / \partial \theta$  and  $\partial \mathbf{u}_k / \partial \theta$ . Given that the system states  $\mathbf{x}_k$  are iteratively defined using the dynamics (1), we can derive an iterative formula for  $\partial \mathbf{x}_k / \partial \theta$  and  $\partial \mathbf{u}_k / \partial \theta$  based on the sensitivity equation of the system [25, Chapter 3.3]:

$$\frac{\partial \mathbf{x}_{k+1}}{\partial \theta} = (\nabla_{\mathbf{x}_k} f + \nabla_{\mathbf{u}_k} f \nabla_{\mathbf{x}_k} h) \frac{\partial \mathbf{x}_k}{\partial \theta} + \nabla_{\mathbf{u}_k} f \nabla_{\theta} h, \quad (5a)$$

$$\frac{\partial \mathbf{u}_k}{\partial \theta} = \nabla_{\mathbf{x}_k} h \frac{\partial \mathbf{x}_k}{\partial \theta} + \nabla_{\theta} h. \quad (5b)$$

The decomposition (4) and sensitivity propagation (5) provide a new perspective to compute the desired gradient  $\nabla_{\theta} L$ . On the one hand, the desired gradient  $\nabla_{\theta} L$  is essentially the weighted sum of the sensitivity  $\partial \mathbf{x}_k / \partial \theta$  and  $\partial \mathbf{u}_k / \partial \theta$ , with the weights given by  $\partial L / \partial \mathbf{x}_k$  and  $\partial L / \partial \mathbf{u}_k$ , respectively, in a window of length  $N$ . Consider an earlier example where  $L(\theta) = \sum_{k=1}^N \|\mathbf{x}_k - \hat{\mathbf{x}}_k\|^2 + \sum_{k=0}^{N-1} \lambda \|\mathbf{u}_k\|^2$ . In this case, the weights are contained in the error vector between the actual and desired state  $\partial L / \partial \mathbf{x}_k = 2(\mathbf{x}_k - \hat{\mathbf{x}}_k)^{\top}$  and the control action itself  $\partial L / \partial \mathbf{u}_k = 2\mathbf{u}_k^{\top}$  at each time step. On the other hand, equations (4)-(5) permit computing the desired gradient  $\nabla_{\theta} L$  using only one forward propagation: no back propagation is required. The sensitivity is propagated along with the dynamics (1) in the forward direction until reaching the end of the window with the intermediate states  $\mathbf{x}_k$ , controls  $\mathbf{u}_k$ , and sensitivities  $\partial \mathbf{x}_k / \partial \theta$  and  $\partial \mathbf{u}_k / \partial \theta$  stored in the memory. The desired gradient  $\nabla_{\theta} L$  is evaluated using decomposition (4) with the stored intermediate values. One will program the dynamics and controller together with the sensitivity equations, with possibly the sensitivity being an augmented state variable itself. In other words, the sensitivity propagation requires all the computations from state update and control action generation to gradient computation to be custom-coded.

*Remark 1:* The sensitivity propagation and backward propagation are equivalent to the forward- and reverse-mode auto-differentiation, respectively, on a computational graph. Thus, both can provide analytical gradients (instead of numerical approximations).

A unique aspect of the sensitivity propagation is its real-data compatibility. Using real data for tuning is vital because

---

**Algorithm 1** DiffTune

---

**Input:** Initial state  $\bar{\mathbf{x}}_0$ , initial parameter  $\theta_0$ , feasible set  $\Theta$ , horizon  $N$ , desired state  $\{\bar{\mathbf{x}}_k\}_{k=0:N}$ , step size  $\alpha$ , and termination condition  $\mathcal{C}$ .

**Output:** Tuned parameter  $\theta^*$

- 1: Initialize  $\theta \leftarrow \theta_0$ .
  - 2: **while**  $\mathcal{C}$  is FALSE **do**
  - 3:   Reset  $\mathbf{x}_0 \leftarrow \bar{\mathbf{x}}_0$ .
  - 4:   **for**  $k \leftarrow 0$  to  $N$  **do**
  - 5:     Obtain  $\mathbf{x}_k$  from system and compute  $\mathbf{u}_k$  using (2).
  - 6:     Update  $\partial \mathbf{x}_{k+1}/\partial \theta$  and  $\partial \mathbf{u}_k/\partial \theta$  using (5).
  - 7:     Compute  $\partial L/\partial \mathbf{x}_k$  and  $\partial L/\partial \mathbf{u}_k$ .
  - 8:     Store  $\mathbf{x}_k$ ,  $\mathbf{u}_k$ ,  $\partial \mathbf{x}_{k+1}/\partial \theta$ ,  $\partial \mathbf{u}_k/\partial \theta$ ,  $\partial L/\partial \mathbf{x}_k$  and  $\partial L/\partial \mathbf{u}_k$  in memory.
  - 9:   **end for**
  - 10:   Compute  $\nabla_{\theta} L$  using (4) and update  $\theta$  by (3).
  - 11: **end while**
  - 12: **return** the tuned parameter  $\theta^* \leftarrow \theta$ .
- 

the ultimate goal is to improve the performance of the real system instead of the simulated system. Despite the preciseness of the model in simulation, the real system will have discrepancies to the model, leading to sub-optimal performance on a real system if the parameters come from simulation-based tuning. This phenomenon is part of the sim-to-real gap which leads to degraded performance on real systems compared to their simulated counterparts. The sensitivity propagation, unlike the back propagation, can still be applied to compute the desired gradient while using data collected from real systems, which will be explained in detail in the next subsection.

### B. Tuning with data from real systems

The core of *DiffTune* is to obtain  $\nabla_{\theta} L$  (from real systems' data, using the decomposition (4) and sensitivity propagation (5)) and then apply projected gradient descent. We summarize the *DiffTune* algorithm in Alg. 1.

However, model uncertainties and noise have to be carefully handled when using data from real systems. Controller design usually uses nominal model of the system, which is uncertainty- and noise-free. However, both uncertainties and noise exist in a real system. If not dealt with, then the uncertainties and noise will contaminate the sensitivity propagation, leading to biased sensitivities and, thus incorrect gradient  $\nabla_{\theta} L$ , which results in inefficient parameter update. Since noise can be efficiently addressed by filtering or state estimation, our focus will be on handling uncertainties.

Existing methods can be applied to mitigate this issue. For example, the  $\mathcal{L}_1$  adaptive control ( $\mathcal{L}_1$ AC) is a robust adaptive control architecture that has the advantage of decoupling estimation from control, thereby allowing for arbitrarily fast adaptation subject only to hardware limitations [38]. It can be applied to make a real system with uncertainties behave like a nominal system by compensating for the uncertainties. To see how  $\mathcal{L}_1$ AC works, consider a control-affine system

$$\dot{\mathbf{x}} = f(\mathbf{x}, t) + B(\mathbf{x}, t)(\mathbf{u} + \mathbf{u}_{ad} + \boldsymbol{\sigma}), \quad (6)$$

where  $\mathbf{x}$ ,  $\mathbf{u}$ ,  $\mathbf{u}_{ad}$ , and  $\boldsymbol{\sigma}$  stand for state, baseline control (of the to-be-tuned controller),  $\mathcal{L}_1$ AC, and uncertainty, respectively. Here,  $\boldsymbol{\sigma}$  is matched uncertainty and we defer the discussion of unmatched uncertainty to future work due to space limitation. The  $\mathcal{L}_1$ AC  $\mathbf{u}_{ad}$  aims to cancel out the uncertainty  $\boldsymbol{\sigma}$ . Intuitively,  $\mathcal{L}_1$ AC compensates for the uncertainties that are lumped from the dynamics as additive terms such that the dynamics of the real system equal to the nominal dynamics plus the additive terms (see [38]–[41] for details of how  $\mathcal{L}_1$ AC is implemented). It can be shown that  $\|\mathbf{u}_{ad} + \boldsymbol{\sigma}\|$  is bounded [42], [43], which renders the uncertain system (6) behaving similar to the nominal system  $\dot{\mathbf{x}} = f(\mathbf{x}, t) + B(\mathbf{x}, t)\mathbf{u}$ . Therefore, the sensitivity propagation remains unchanged while  $\mathcal{L}_1$ AC handles the uncertainties. We will illustrate how the  $\mathcal{L}_1$ AC facilitates the tuning in Section V.

## V. SIMULATION RESULTS

In this section, we implement *DiffTune* for a Dubin's car and a quadrotor in simulations, where the controller in each case is differentiable. For all simulations, we use the sensitivity propagation to compute  $\nabla_{\theta} L$ , use the forward-Euler method to discretize the dynamics for sensitivity propagation, and use `ode45` to obtain the system states by integrating the continuous-time dynamics (mimicking the continuous-time physical process on a real system).

### A. Dubin's car

**Formulation:** Consider the following nonlinear model:

$$\dot{x}(t) = v(t) \cos(\psi(t)), \quad \dot{y}(t) = v(t) \sin(\psi(t)), \quad (7a)$$

$$\dot{\psi}(t) = \omega(t), \quad \dot{v}(t) = F(t)/m, \quad \dot{w}(t) = M(t)/J, \quad (7b)$$

where the state contains five scalar variables,  $(x, y, \psi, v, w)$ , which stand for horizontal position, vertical position, yaw angle, linear speed in the forward direction, and angular speed. The control actions in this model include the force  $F \in \mathbb{R}$  on the forward direction of the vehicle and the moment  $M \in \mathbb{R}$ . The vehicle's mass and moment of inertia are known and denoted by  $m$  and  $J$ , respectively. The feedback tracking controller with learnable parameter  $\theta = (k_{\mathbf{p}}, k_{\mathbf{v}}, k_{\psi}, k_{\omega})$  is given by

$$F(t) = m(k_{\mathbf{p}}\mathbf{e}_{\mathbf{p}}(t) + k_{\mathbf{v}}\mathbf{e}_{\mathbf{v}}(t) + \hat{\dot{\mathbf{v}}}(t)) \cdot \mathbf{q}(t), \quad (8a)$$

$$M(t) = J(k_{\psi}e_{\psi}(t) + k_{\omega}e_{\omega}(t) + \hat{\dot{\omega}}(t)), \quad (8b)$$

where  $\hat{\cdot}$  indicates the desired value, the error terms are defined by  $\mathbf{e}_{\mathbf{p}} = \hat{\mathbf{p}} - \mathbf{p}$ ,  $\mathbf{e}_{\mathbf{v}} = \hat{\mathbf{v}} - \mathbf{v}$ ,  $e_{\psi} = \hat{\psi} - \psi$ , and  $e_{\omega} = \hat{\omega} - \omega$  for  $\mathbf{p}$  and  $\mathbf{v}$  being the 2-dimensional vector of position and velocity, respectively,  $\mathbf{q} = [\cos(\psi) \quad \sin(\psi)]^{\top}$  being the heading of the vehicle,  $\hat{\mathbf{v}} = [\hat{v} \cos(\psi) \quad \hat{v} \sin(\psi)]^{\top}$  and  $\hat{\dot{\mathbf{v}}}$  being the desired linear velocity and acceleration, respectively. The control law (8) is a PD controller with proportional gains  $(k_{\mathbf{p}}, k_{\psi})$  and derivative gains  $(k_{\mathbf{v}}, k_{\omega})$ . If  $\theta > 0$ , then this controller is exponentially stable for the tracking errors  $(\|\mathbf{e}_{\mathbf{p}}\|, \|\mathbf{e}_{\mathbf{v}}\|, \|e_{\psi}\|, \|e_{\omega}\|)$ .

**Simulation setup:** The loss function is the squared norm of the position tracking error, summed over a horizon of 10 s.

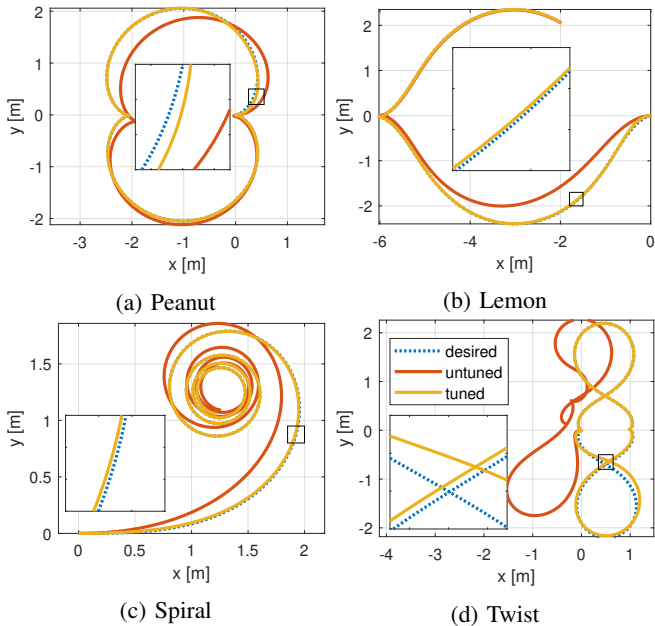


Fig. 2: Testing trajectories and the performance comparison between tuned and untuned controller parameters.

We choose 0.1 as the step size in the gradient descent algorithm and choose the termination condition as the relative reduction in the total loss between two consecutive steps being smaller than  $1e-4$  of the current loss value.

**Generalizability:** We first illustrate the generalizability of *DiffTune*. We select nine trajectories as the training set, where these trajectories have the maximum linear speed and angular speed of 1 m/s and 1 rad/s, respectively, to represent trajectories in one operating region. The four control parameters are all initialized at 2. The tuning proceeds by batch gradient descent on the training set. The controller parameters converge to  $(k_p, k_v, k_\psi, k_\omega) = (18.83, 6.69, 14.97, 2.66)$ . We then test the tuned parameters on four testing trajectories (unseen in the training set) with lemon-, twist-, peanut-, and spiral-shape, as shown in Fig. 2. The tuned parameters lead to better tracking performance than the untuned ones. The loss on the testing set are compared to the untuned parameters in Table I. It can be observed that the tuned parameters generalize well and are robust to the previously unseen trajectories.

TABLE I: Testing trajectories for Dubin’s car simulation and associated loss. The average loss of the tuned parameters on the training set is 0.36.

Trajectory	max speed		loss	
	linear	angular	w/ <i>DiffTune</i>	w/o <i>DiffTune</i>
peanut	2	1.3	<b>0.07</b>	55.18
lemon	2	1	<b>2.05</b>	974.57
spiral	1	5	<b>0.18</b>	63.02
twist	2	3.4	<b>0.39</b>	21.11

**Handling uncertainties:** In the second simulation, we implement the  $\mathcal{L}_1$ AC to facilitate the system compensating for the uncertainties during tuning. For the  $\mathcal{L}_1$ AC, we use the piecewise-constant adaptation law and a 1st-order low-pass filter with 20 rad/s bandwidth. In this simulation, we inject additive force  $0.1a_1 \sin(t)$  and moment  $0.1a_2 \cos(t)$  to the

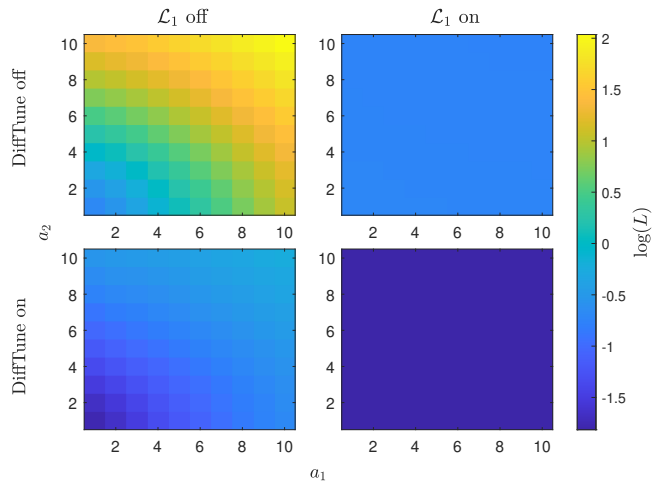


Fig. 3: Loss  $L$  subject to uncertainties (additive force  $0.1a_1 \sin(t)$  and moment  $0.1a_2 \cos(t)$ ) in the ablation study of *DiffTune* and  $\mathcal{L}_1$ AC.

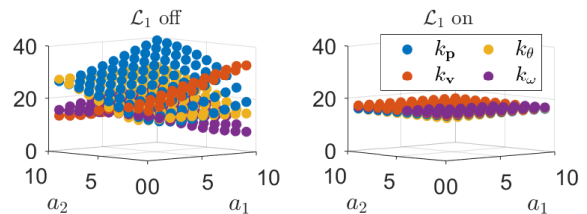


Fig. 4: Tuned controller parameters subject to uncertainties (additive force  $0.1a_1 \sin(t)$  and moment  $0.1a_2 \cos(t)$ ).

control channels in the dynamics (7) as uncertainties from the environment. To understand how the tuned parameters alter based on different amplitude of the uncertainties, we set  $(a_1, a_2)$  to a  $10 \times 10$  grid such that  $a_1$  and  $a_2$  take integer values from 1 to 10. The four control parameters are all initialized at 10. We tune the controller parameters with both  $\mathcal{L}_1$  on and  $\mathcal{L}_1$  off, where the sensitivity propagation in both cases is based on the nominal model in (7). Different from the training-test scenario in the previous simulation, we only tune the parameters on one trajectory (the focus is how to reduce the impact of the uncertainties that are not considered in the nominal dynamics). The step size and termination criterion remain the same as before. To clearly understand the individual role by *DiffTune* and the  $\mathcal{L}_1$ AC, we conduct an ablation study. The losses are shown in Fig. 3. It can be observed that both *DiffTune* and  $\mathcal{L}_1$ AC improve the performance: the  $\mathcal{L}_1$ AC does so by compensating for the uncertainties, whereas *DiffTune* does so by driving the parameters to achieve smaller tracking error. Although the two heatmaps with  $\mathcal{L}_1$  on show indistinguishable color within each itself, the actual loss values have minor fluctuations. Figure 4 shows the tuned parameters when  $\mathcal{L}_1$  is off and on. The influence of uncertainties to tuning is clear in that when  $\mathcal{L}_1$  is off, the controller itself needs to counteract the uncertainties by significantly raising the gains, resulting in uncertainty-dependent values. For each case of the uncertainty, the converged gains can achieve case-specific satisfactory performance, leading to undesirable performance

if the uncertainties alter away from the one during tuning. Furthermore, the large gains will sacrifice the system's robustness by amplifying the noise into the control channel. Contrarily, when  $\mathcal{L}_1$  compensates for the uncertainties, the tuning can be done to the "nominal dynamics," yielding consistent parameter values that are less affected by uncertainties.

### B. Quadrotor

**Formulation:** Consider the following model on  $SE(3)$ :

$$\dot{\mathbf{p}} = \mathbf{v}, \quad \dot{\mathbf{v}} = g\mathbf{e}_3 - \frac{f}{m}R\mathbf{e}_3, \quad (9a)$$

$$\dot{R} = R\Omega^\times, \quad \dot{\Omega} = J^{-1}(\mathbf{M} - \Omega \times J\Omega), \quad (9b)$$

where  $\mathbf{p} \in \mathbb{R}^3$  and  $\mathbf{v} \in \mathbb{R}^3$  are the position and velocity of the quadrotor, respectively,  $R \in SO(3)$  is the rotation matrix describing the quadrotor's attitude,  $\Omega \in \mathbb{R}^3$  is the angular velocity,  $g$  is the gravitational acceleration,  $m$  is the vehicle mass,  $J \in \mathbb{R}^{3 \times 3}$  is the moment of inertia (MoI) matrix,  $f$  is the collective thrust, and  $\mathbf{M} \in \mathbb{R}^3$  is the moment applied to the vehicle. The *wedge* operator  $\cdot^\times : \mathbb{R}^3 \rightarrow \mathfrak{so}(3)$  denotes the mapping to the space of skew-symmetric matrices. The control actions  $f$  and  $\mathbf{M}$  are computed using the geometric controller [44], with the simplification that the desired angular rate  $\hat{\Omega} = 0$ . The geometric controller has a 12-dimensional parameter space, which splits into four groups of parameters:  $\mathbf{k}_p$ ,  $\mathbf{k}_v$ ,  $\mathbf{k}_R$ ,  $\mathbf{k}_\Omega$  (applying to the tracking errors in position, linear velocity, attitude, and angular velocity, respectively). Each group is a 3-dimensional vector (associated with the  $x$ -,  $y$ -, and  $z$ -component in each's corresponding tracking error). The initial parameters for tuning are set as  $\mathbf{k}_p = 16\mathbb{I}$ ,  $\mathbf{k}_v = 5.6\mathbb{I}$ ,  $\mathbf{k}_R = 8.81\mathbb{I}$ , and  $\mathbf{k}_\Omega = 2.54\mathbb{I}$ , for  $\mathbb{I} = [1, 1, 1]^\top$ . We add zero-mean Gaussian noise to the position, linear velocity, and angular velocity (with standard deviation 0.1 m, 0.1 m/s, 1e-3 rad/s, respectively).

**Simulation setup:** We use the desired trajectory for tuning:  $\hat{\mathbf{p}}(t) = [2(1 - \cos(t)), 2(\cos(t) - 1), 0]^\top$  with a constant desired yaw angle at 0 (the quadrotor's differentially flat dynamics enable the description of the desired state by position and yaw and their derivatives [45]). The loss function is the squared norm of the position tracking error, summed over a horizon of 10 s. We choose 1e-3 as the step size in the gradient descent algorithm. The termination condition is either the relative loss reduction being less than 1e-3 of the current loss value or the current loss increasing by more than 10% of the previous loss. We set the 10% threshold to tolerate loss oscillation by the noisy data and avoid an early termination.

**Handling uncertainties:** In this simulation, we consider the uncertainty caused by the imprecisely known value  $J$  of the MoI. We set the vehicle's true MoI as  $\beta J$  for  $\beta$  from 0.5 to 4 and use  $J$  in the controller design as our best knowledge of the system. The scaled MoI can be treated as an unknown control input gain (see (9b)), leading to decreased ( $\beta > 1$ ) or increased ( $\beta < 1$ ) moment in reality compared to the commanded moment by the geometric

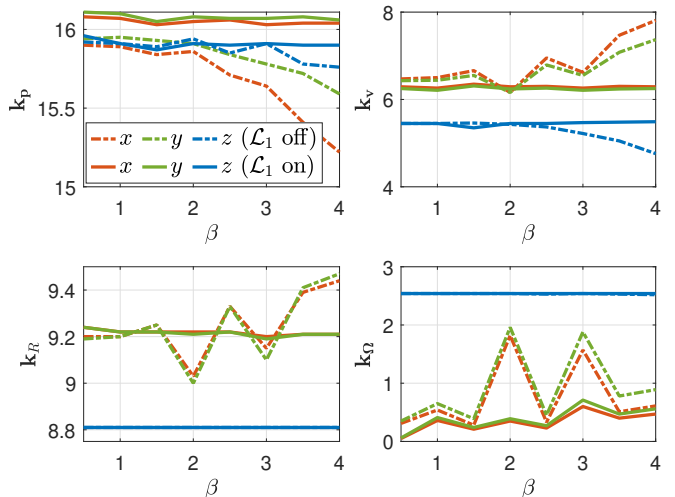


Fig. 5: Tuned parameters  $\mathbf{k}_p$ ,  $\mathbf{k}_v$ ,  $\mathbf{k}_R$ , and  $\mathbf{k}_\Omega$  for the geometric controller of a quadrotor. The uncertainties are introduced by the mismatch on the moment of inertia between the controller's knowledge  $J$  and the true value  $\beta J$ .

controller. However, the uncertainty caused by the perturbed MoI can be well handled by  $\mathcal{L}_1$ AC, which is adopted in the simulation (formulation detailed in [39]). We conduct an ablation study to understand the roles by *DiffTune* and  $\mathcal{L}_1$ AC by comparing the root-mean-square error (RMSE) of position tracking, as shown in Table II. It can be seen that tuning and  $\mathcal{L}_1$  can individually reduce the tracking RMSE. The best performance is achieved when tuning and  $\mathcal{L}_1$ AC are applied jointly, despite almost indistinguishable inferior performance caused by the noise when  $\beta = 0.5$  and 1. We show the tuned controller parameters in Fig. 5. The parameters with  $\mathcal{L}_1$  in the loop show better consistency than those without  $\mathcal{L}_1$  across the perturbation on the MoI. This observation is consistent with that in the Dubin's car simulation (Fig. 4).

TABLE II: Tracking RMSE [cm] with MoI perturbation  $\beta$  ranging from 0.5 to 4. (T stands for "DiffTune.")

T	$\mathcal{L}_1$	0.5	1	1.5	2	2.5	3	3.5	4
✓	✓	17.7	18.3	<b>17.9</b>	<b>18.0</b>	<b>18.4</b>	<b>18.5</b>	<b>18.4</b>	<b>18.4</b>
✓	✗	<b>17.6</b>	<b>18.0</b>	18.0	25.7	19.9	23.9	21.1	22.3
✗	✓	36.9	37.0	37.0	36.5	36.1	36.3	35.7	35.0
✗	✗	35.5	35.7	37.3	38.8	40.9	41.8	44.4	45.6

## VI. CONCLUSION

In this paper, we propose *DiffTune*: an auto-tune method for controller tuning in systems with differentiable dynamics and controller. Given a performance metric, *DiffTune* gradually improves the performance using gradient-descent, where the gradient is computed using the sensitivity propagation that is compatible with real-data. We also discuss how to use  $\mathcal{L}_1$ AC to mitigate the discrepancy between the nominal model and the real system when the latter suffers from uncertainties. Simulation results on the Dubin's car and the quadrotor show that *DiffTune* improves the system's performance while  $\mathcal{L}_1$ AC compensates for the uncertainties. Generalizability of the tuned parameters is also illustrated using training and test sets in the Dubin's car simulation.

## REFERENCES

- [1] A. O’Dwyer, *Handbook of PI and PID controller tuning rules*. Singapore: World Scientific, 2009.
- [2] C.-C. Yu, *Autotuning of PID controllers: A relay feedback approach*. Berlin, Germany: Springer, 2006.
- [3] K. J. Åström, T. Hägglund, C. C. Hang, and W. K. Ho, “Automatic tuning and adaptation for PID controllers - a survey,” *Control Engineering Practice*, vol. 1, no. 4, pp. 699–714, 1993.
- [4] Y. Li, K. H. Ang, and G. C. Chong, “Patents, software, and hardware for PID control: an overview and analysis of the current art,” *IEEE Control Systems Magazine*, vol. 26, no. 1, pp. 42–54, 2006.
- [5] M. Zhuang and D. Atherton, “Automatic tuning of optimum PID controllers,” in *IEE Proceedings D (Control Theory and Applications)*, vol. 140, no. 3. IET Digital Library, 1993, pp. 216–224.
- [6] S. Trimpe, A. Millane, S. Doessegger, and R. D’Andrea, “A self-tuning LQR approach demonstrated on an inverted pendulum,” *IFAC Proceedings Volumes*, vol. 47, no. 3, pp. 11 281–11 287, 2014.
- [7] A. R. Kumar and P. J. Ramadge, “DiffLoop: Tuning PID controllers by differentiating through the feedback loop,” in *Proceedings of the 55th Annual Conference on Information Sciences and Systems*, Baltimore, MD, USA, 2021, pp. 1–6.
- [8] A. Marco, P. Hennig, J. Bohg, S. Schaal, and S. Trimpe, “Automatic LQR tuning based on Gaussian process global optimization,” in *Proceedings of IEEE International Conference on Robotics and Automation*, Stockholm, Sweden, 2016, pp. 270–277.
- [9] F. Berkenkamp, A. P. Schoellig, and A. Krause, “Safe controller optimization for quadrotors with Gaussian processes,” in *Proceedings of IEEE International Conference on Robotics and Automation*, Stockholm, Sweden, 2016, pp. 491–496.
- [10] R. Calandra, N. Gopalan, A. Seyfarth, J. Peters, and M. P. Deisenroth, “Bayesian gait optimization for bipedal locomotion,” in *Proceedings of the International Conference on Learning and Intelligent Optimization*, Gainesville, FL, USA, 2014, pp. 274–290.
- [11] D. J. Lizotte, T. Wang, M. H. Bowling, D. Schuurmans *et al.*, “Automatic gait optimization with Gaussian Process Regression,” in *Proceedings of the International Joint Conferences on Artificial Intelligence Organization*, vol. 7, Hyderabad, India, 2007, pp. 944–949.
- [12] A. Loquercio, A. Saviolo, and D. Scaramuzza, “Autotune: Controller tuning for high-speed flight,” *IEEE Robotics and Automation Letters*, vol. 7, no. 2, pp. 4432–4439, 2022.
- [13] M. Mehndiratta, E. Camci, and E. Kayacan, “Can deep models help a robot to tune its controller? A step closer to self-tuning model predictive controllers,” *Electronics*, vol. 10, no. 18, p. 2187, 2021.
- [14] C. K. Williams and C. E. Rasmussen, *Gaussian Processes for Machine Learning*. Cambridge, MA, USA: MIT press, 2006, vol. 2, no. 3.
- [15] B. Amos and J. Z. Kolter, “OptNet: Differentiable optimization as a layer in neural networks,” in *Proceedings of the 34th International Conference on Machine Learning*, Sydney, Australia, 2017, pp. 136–145.
- [16] B. Amos, I. Jimenez, J. Sacks, B. Boots, and J. Z. Kolter, “Differentiable MPC for end-to-end planning and control,” in *Proceedings of the 32nd Conference on Neural Information Processing Systems*, vol. 31, Montreal, Canada, 2018.
- [17] S. East, M. Gallieri, J. Masci, J. Koutnik, and M. Cannon, “Infinite-horizon differentiable model predictive control,” in *Proceedings of the International Conference on Learning Representations*, Online, 2020.
- [18] W. Jin, Z. Wang, Z. Yang, and S. Mou, “Pontryagin differentiable programming: An end-to-end learning and control framework,” in *Proceedings of the 34th Conference on Neural Information Processing Systems*, vol. 33, Vancouver, Canada, 2020, pp. 7979–7992.
- [19] W. Jin, T. D. Murphey, D. Kulić, N. Ezer, and S. Mou, “Learning from sparse demonstrations,” *IEEE Transactions on Robotics*, 2022.
- [20] H. Ma, B. Zhang, M. Tomizuka, and K. Sreenath, “Learning differentiable safety-critical control using control barrier functions for generalization to novel environments,” *arXiv:2201.01347*, 2022.
- [21] W. Xiao, R. Hasani, X. Li, and D. Rus, “BarrierNet: A safety-guaranteed layer for neural networks,” *arXiv:2111.11277*, 2021.
- [22] W. Xiao, T.-H. Wang, M. Chahine, A. Amini, R. Hasani, and D. Rus, “Differentiable control barrier functions for vision-based end-to-end autonomous driving,” *arXiv:2203.02401*, 2022.
- [23] H. Parwana and D. Panagou, “Recursive feasibility guided optimal parameter adaptation of differential convex optimization policies for safety-critical systems,” *arXiv:2109.10949*, 2021.
- [24] N. A. Vien and G. Neumann, “Differentiable robust LQR layers,” *arXiv:2106.05535*, 2021.
- [25] H. K. Khalil, *Nonlinear Control*. London, United Kingdom: Pearson, 2015, vol. 406.
- [26] J. C. Spall, *Introduction to Stochastic Search and Optimization: Estimation, Simulation, and Control*. Hoboken, NJ, USA: Wiley, 2005.
- [27] N. J. Killingsworth and M. Krstic, “PID tuning using extremum seeking: online, model-free performance optimization,” *IEEE Control Systems Magazine*, vol. 26, no. 1, pp. 70–79, 2006.
- [28] W. Edwards, G. Tang, G. Mamakoukas, T. Murphey, and K. Hauser, “Automatic tuning for data-driven model predictive control,” in *Proceedings of the IEEE International Conference on Robotics and Automation*, Xi’an, China, 2021, pp. 7379–7385.
- [29] A. S. Polydoros and L. Nalpantidis, “Survey of model-based reinforcement learning: Applications on robotics,” *Journal of Intelligent & Robotic Systems*, vol. 86, no. 2, pp. 153–173, 2017.
- [30] F. Tambon, G. Laberge, L. An, A. Nikanjam, P. S. N. Mindom, Y. Pequignot, F. Khomh, G. Antonioli, E. Merlo, and F. Laviolette, “How to certify machine learning based safety-critical systems? A systematic literature review,” *Automated Software Engineering*, vol. 29, no. 2, pp. 1–74, 2022.
- [31] H. Ravichandar, A. S. Polydoros, S. Chernova, and A. Billard, “Recent advances in robot learning from demonstration,” *Annual Review of Control, Robotics, and Autonomous Systems*, vol. 3, pp. 297–330, 2020.
- [32] J.-X. Xu, “A survey on iterative learning control for nonlinear systems,” *International Journal of Control*, vol. 84, no. 7, pp. 1275–1294, 2011.
- [33] D. A. Bristow, M. Tharayil, and A. G. Alleyne, “A survey of iterative learning control,” *IEEE control systems magazine*, vol. 26, no. 3, pp. 96–114, 2006.
- [34] L. Brunke, M. Greeff, A. W. Hall, Z. Yuan, S. Zhou, J. Panerati, and A. P. Schoellig, “Safe learning in robotics: From learning-based control to safe reinforcement learning,” *Annual Review of Control, Robotics, and Autonomous Systems*, vol. 5, pp. 411–444, 2022.
- [35] N. Parikh, S. Boyd *et al.*, “Proximal algorithms,” *Foundations and Trends® in Optimization*, vol. 1, no. 3, pp. 127–239, 2014.
- [36] A. Paszke, S. Gross, F. Massa, A. Lerer, J. Bradbury, G. Chanan, T. Killeen, Z. Lin, N. Gimelshein, L. Antiga, A. Desmaison, A. Kopf, E. Yang, Z. DeVito, M. Raison, A. Tejani, S. Chilamkurthy, B. Steiner, L. Fang, J. Bai, and S. Chintala, “PyTorch: An imperative style, high-performance deep learning library,” in *Proceedings of the 33rd Conference on Neural Information Processing Systems*, Vancouver, Canada, 2019, pp. 8024–8035.
- [37] M. Abadi, A. Agarwal, P. Barham, E. Brevdo, Z. Chen, C. Citro, G. S. Corrado, A. Davis, J. Dean, M. Devin, S. Ghemawat, I. Goodfellow, A. Harp, G. Irving, M. Isard, Y. Jia, R. Jozefowicz, L. Kaiser, M. Kudlur, J. Levenberg, D. Mané, R. Monga, S. Moore, D. Murray, C. Olah, M. Schuster, J. Shlens, B. Steiner, I. Sutskever, K. Talwar, P. Tucker, V. Vanhoucke, V. Vasudevan, F. Viégas, O. Vinyals, P. Warden, M. Wattenberg, M. Wicke, Y. Yu, and X. Zheng, “TensorFlow: Large-scale machine learning on heterogeneous systems,” *arXiv:1603.04467*, 2016.
- [38] N. Hovakimyan and C. Cao,  *$\mathcal{L}_1$  Adaptive Control Theory: Guaranteed Robustness with Fast Adaptation*. Philadelphia, PA, USA: SIAM, 2010.
- [39] Z. Wu, S. Cheng, K. A. Ackerman, A. Gahlawat, A. Lakshmanan, P. Zhao, and N. Hovakimyan, “ $\mathcal{L}_1$  adaptive augmentation for geometric tracking control of quadrotors,” in *Proceedings of the International Conference on Robotics and Automation*, Philadelphia, PA, USA, 2022, pp. 1329–1336.
- [40] J. Pravitra, K. A. Ackerman, C. Cao, N. Hovakimyan, and E. A. Theodorou, “ $\mathcal{L}_1$ -adaptive MPPI architecture for robust and agile control of multirotors,” in *Proceedings of the IEEE/RSJ International Conference on Intelligent Robot and Systems*, Las Vegas, NV, USA, 2020.
- [41] D. Hanover, P. Foehn, S. Sun, E. Kaufmann, and D. Scaramuzza, “Performance, precision, and payloads: Adaptive nonlinear MPC for quadrotors,” *IEEE Robotics and Automation Letters*, vol. 7, no. 2, pp. 690–697, 2021.
- [42] X. Wang and N. Hovakimyan, “ $\mathcal{L}_1$  adaptive controller for nonlinear time-varying reference systems,” *Systems & Control Letters*, vol. 61, no. 4, pp. 455–463, 2012.

- [43] A. Gahlawat, A. Lakshmanan, L. Song, A. Patterson, Z. Wu, N. Hovakimyan, and E. A. Theodorou, "Contraction  $\mathcal{L}_1$ -adaptive control using Gaussian processes," in *Proceedings of the 3rd Conference on Learning for Dynamics and Control*, vol. 144, Online, 07 – 08 June 2021, pp. 1027–1040.
- [44] T. Lee, M. Leok, and N. H. McClamroch, "Geometric tracking control of a quadrotor UAV on SE(3)," in *Proceedings of the 49th IEEE Conference on Decision and Control*, Atlanta, GA, USA, 2010, pp. 5420–5425.
- [45] D. Mellinger and V. Kumar, "Minimum snap trajectory generation and control for quadrotors," in *Proceedings fo the International Conference on Robotics and Automation*, Shanghai, China, 2011, pp. 2520–2525.